BJRS

BRAZILIAN JOURNAL
OF
RADIATION SCIENCES
08-01A (2020) 01-10

Impact of infill percentages in visual homogeneity for 3D printed imaging phantoms

Andrade[a] M.A.B., Savi[a,b] M., Alves[a] C.O., Fin[a] A.P.C., Soares[a] F.A.P., Potiens[b] M.P.A.

[a] *Instituto Federal de Educação, Ciência e Tecnologia de SC - IFSC, Florianópolis, SC, Brazil*

[b] *Instituto de Pesquisas Energéticas Nucleares - IPEN, São Paulo-SP, Brazil*

marco.bertoncini@ifsc.edu.br

ABSTRACT

The main goal of a 3D printed imaging phantom is to attenuate the radiation in order to differentiate tissues of the human body. This paper aims to verify the infill printing parameter in relation to its final homogeneity in printed samples. Sixteen 8 cm³ cubes with 15% to 90% infill variation, with 5% increments, were printed on PLA + Copper (Cu) and pure ABS. The samples were irradiated using a CT scan at 120 kV, 200 mA, 0.4 mm sections and reconstructed with standard filter. For each cube the mean values of Hounsfield Units (HU) and standard deviation (SD) in a Region of Interest (ROI) were determined. Visually, the internal lattice of each cube was assessed by counting line pairs per millimeter (lp/mm) using a DICOM viewer. Infill values above 50% for PLA + Cu and 55% for ABS showed a high homogeneity that does not allow line pair differentiation. In conclusion, values above and including the found percentages are recommended for use in construction of imaging phantoms.

Keywords: **3D printing, radiology, imaging phantom,**

ISSN: 2319-0612
Accepted: 2020-02-20

1. INTRODUCTION

The process of 3D printing consists in creating three-dimensional objects by successively depositing 2D layered materials [1]. Created by Charles Hull in 1986 [2], 3D printers were adopted by the automotive and aerospace industry to create test prototypes before proceeding with mass production. In the 2000s, 3D printers gained ground in the medical field with prototyping of dental implants, anatomical models and bolus radiotherapy [3,4].

There are currently several 3D printers models and technologies on the market and the most commonly used is Fused Filament Fabrication (FFF) technology, that often uses thermoplastic materials such as ABS (acrylonitrile butadiene styrene) and PLA (polylactic acid) in layer-by-layer deposition [5]. Also, 3D printing technology is able to create objects with complex internal structures, with greater versatility and customization [6] and when combined with medical images, produces anatomical models from patient data to enable visualization of complicated pathologies or even enable the creation of custom prostheses and implants [7]. The 3D printing of anatomical models from medical images is being used in the manufacture of organs, living tissues, as well as in the pharmaceutical area [8,9], however, the cost and time required to produce products by this technology still limit its wide use in hospitals and research [10,11].

In radiology, 3D printing can be presented as an alternative for the development of radiographic phantoms, to be used in the optimization of techniques and images [12], quality control of radiographs and equipments, in the aid of teaching and research and in radiological protection programs [13-15], by simulating radiation attenuation and mimicking the different tissues of the human body.

Quality control of radiological equipment commonly uses imaging phantoms to ensure quality and performance excellence [16]. Phantoms are also used in medicine and related areas because they represent the human body, from simpler forms such as water simulators, to complex ones, such as anthropomorphic ones, and have become essential in both imaging and dosimetric areas [17], as the literature reports use of 3D printing to develop phantoms for this purpose [18-20].

The 3D printed anthropomorphic phantoms are constructed based on computed tomography or magnetic resonance imaging, so that organs and tissues are segmented according to different density levels depicted in the HU values or signal strength.

Based on the premise that 3D printing technology can contribute to the production of imaging phantoms, this study seeks to verify the influence of the infill printing parameter on the final homogeneity of printed samples [22], which can be verified by the visual perception of lines or patterns when producing a medical image. In the use of 3D printing technology, it is common to vary the fill patterns and densities, thus reducing printing time and material consumption [23] and, in radiological uses, changing the linear attenuation of the printed sample [24].

2. MATERIALS AND METHODS

In order to carry out the visual homogeneity assessment, the line pair count per millimeter (lp/mm) was used to determine the spatial resolution, also being a comparison parameter to assess the feasibility of using the studied materials [14, 21]. Sixteen 8 cm^3 cubes with internal rectilinear infill pattern (+45° and -45°) were printed using two different materials, being PLA (polylactic acid) with 27.5 ± 2.5% copper (Cu) manufactured by UP3D© and pure ABS (acrylonitrile butadiene styrene) manufactured by 3DON©, totaling 32 cubes. These materials were chosen for their ability to mimic different types of soft tissue, such as skin, adipose tissue, among others, depending on the percentage of filling [25]. The infill variation range was defined between 15% to 90%, with 5% increments. The extrusion diameter used was 0.4 mm and the height of each print layer is about 0.2 mm on a FFF technology Flashforge Creator Pro 3D printer.

Figure 1:*Arrangement of samples on tomography examination table.*

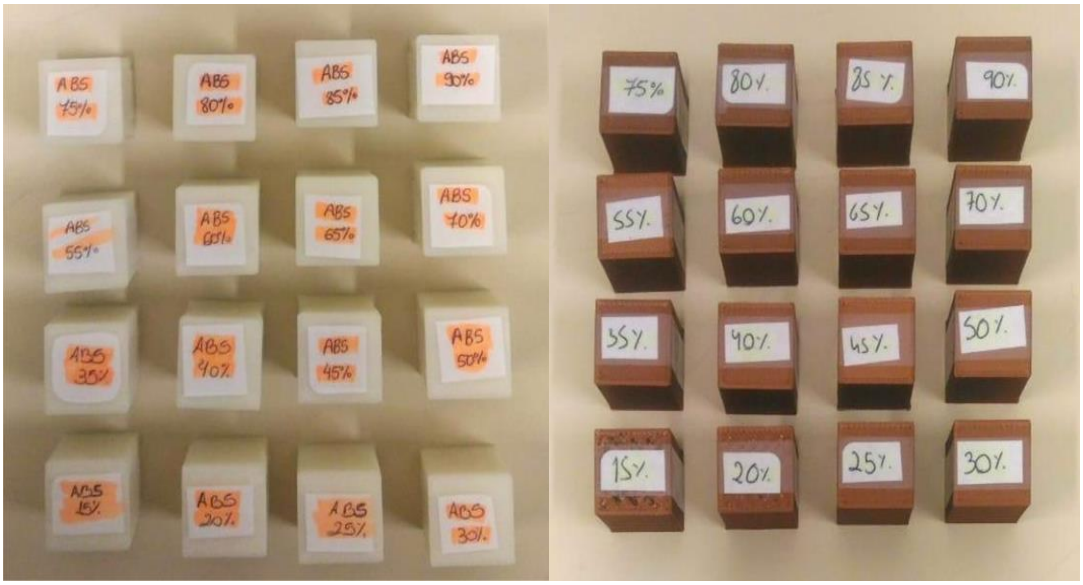

The internal visual evaluation of the cubes was performed on a 6-channel Philips Brilliance CT scanner using 120 kVp, 200 mA, helicoidal mode with 0.8 mm slices and standard reconstruction algorithm. For this assay, the samples were organized in two groups on the examination table, separated by filament type and arranged in two 4 by 4 matrices, with approximate spacing of 1 cm between cubes.

The mean values of Hounsfield Units (HU) and standard deviation (SD) were determined in a Region of Interest (ROI) of 113.4 mm² and the internal lattice of each cube was evaluated in terms of lp/mm using the viewer DICOM Weasis.

3. RESULTS AND DISCUSSION

Figures 2 and 3 show that visual homogeneity of printed samples is achieved with infill values above 50% for PLA + Cu and 55% for ABS, since higher values do not allow line pair differentiation. The resolution value for PLA + Cu ranged from 0.233 lp/mm at 15% infill and 0.714 lp/mm at 45% infill. For the samples produced in ABS, the variation was between 0.233 lp/mm for 15% and 0.769 lp/mm for 50% infill. It was also possible to confirm, as shown in Figure 4, that the HU values present a behavior that evolves with the increase in the infill value, due to the

increase of samples density. It is important to highlight the growth of standard deviation as the infill diminishes, especially for values below 45%. This growth can be explained by the raising of air filled spaces, which leads to a larger distribution of HU of the pixels.

Figure 2: *Measurements on 15% to 50% infill, PLA+Cu.*

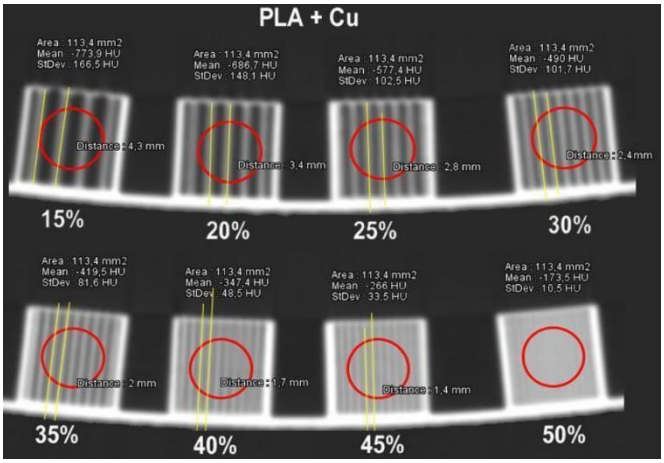

Figure 3: *Measurements on 15% to 50% infill samples, ABS.*

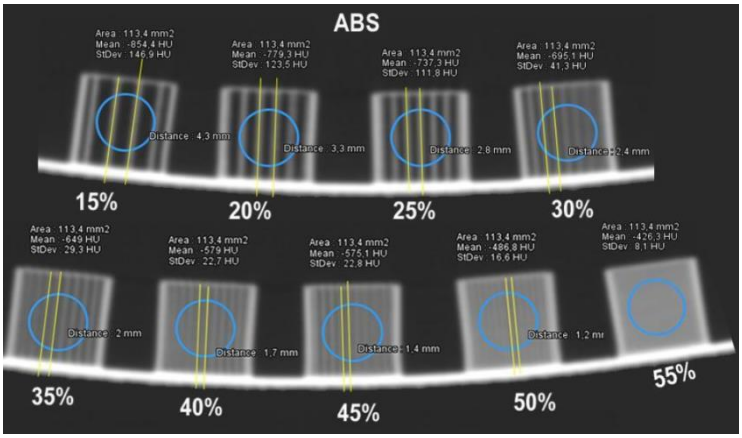

It was also noticed that the result of lp/mm in the rectilinear infill pattern is fixed for each fill percentage, regardless of the material to be used. Thus, the 15% fill percentage provides internal lines 4.3 mm apart, equivalent to 0.233 lp/mm, because the printing software that plans the path taken by the extruder estimates that such a value is sufficient to physically fill the part at a 1 to

6.666 ratio (15%). As the infill value increases the rectilinear lines get closer to each other, and due to resolution limitations of the CT equipment and intrinsic aspects of the material used, they become less discernible.

Figure 4: *HU values evolution in relation to the infill percentages.*

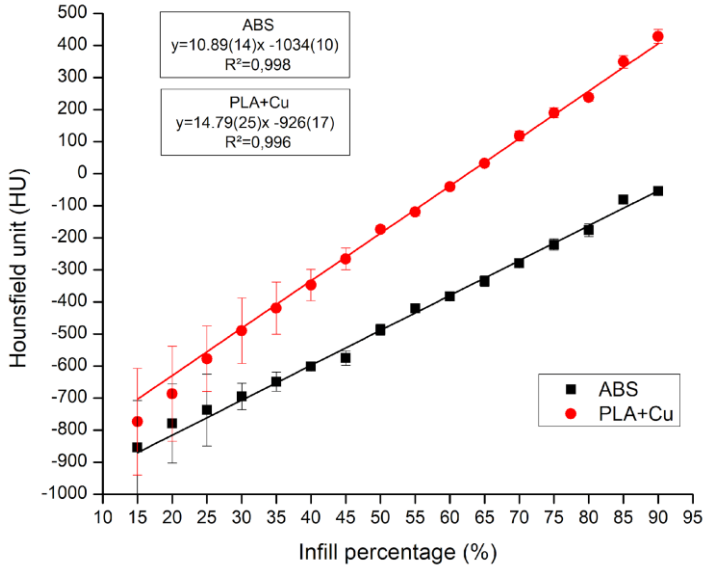

Characteristic HU values for air are around -1000, for lung from -500 to -200, adipose tissue -200 to -20, water 0, blood 25, muscle 25 to 40, liver 45 to 65, soft tissue between 20 and 100, trabecular bone tissue between 200 and 400 and compact bone from 401 to 1000 [26, 27]. According to the HU values found in the assays, the PLA + Cu material is capable of representing homogeneous lung tissue (HU-173.5) with at least 50% infill, and trabecular bone tissue (HU 428.2) with at least 90% infill. For ABS material, the tissues that can be represented range between the lung tissue (HU -420.6) with a 55% infill and adipose tissue (HU -54.4) with a 90% infill.

The infill's homogeneity of materials used in imaging phantoms is essential for the differentiation of tissues and organs of the human body, enabling the production of patient-specific phantoms for use in dosimetry or radiotherapy treatments, where the phantom may require geometry accuracy and sufficient tissue equivalent to provide realistic measurements of radiation effects [28].

4. CONCLUSION

Infill percentage is one of the most important parameters that can be chosen when a 3D printed object is made. This paper brings to light the limitation behind infill percentage selection to homogeneity in a CT image, defining the lowest value that can be used to 3D print a phantom using two materials. It was visually noticed that PLA + Cu filament with infill percentages above 50% and 55% for ABS are indicated to produce 3D printing imaging phantoms. Values below of the presented may produce noticeable line pairs, causing the sample to lose visual homogeneity and consequent tissue mimicry. Within this homogeneous infill percentages, it is possible to simulate different soft tissues types in the construction of imaging phantoms. Despite the relatively small variation between materials observed in the results, more studies should be conducted aiming to evaluate other filaments, with different compositions, to increase the range of body tissues that can be mimicked using 3D printing FFF technology.

ACKNOWLEDGMENT

The authors would like to thank IFSC, IPEN, CAPES, FAPESP (PROJECT 2017/50332-0) and CNPq (PROJECT 312131/2016-0) for the partial financial support.

REFERENCES

[1] MARRO, A., BANDUKWALA, T., MAK, W. Three-dimensional printing and medical imaging: A review of the methods and applications. **Elsevier**, v. 45, p. 2-9, 2016. Available at: https://www.sciencedirect.com/science/article/pii/S0363018815001127

[2] HULL, C. Aparelho para Produção de Objetos Tridimensionais por Estereolitografia 1986. Available at: https://patents.google.com/patent/US4575330A/en

[3] VENTOLA, C. Medical Applications for 3D Printing: Current and Projected Uses. **P&T**, v. 39, p. 704 – 711, 2014.

[4] HESPEL, A.; WILHITE, R.; HUDSON, J. Invited review – Applications for 3D printers in veterinary medicine, **Vet Radiology and Ultrasound**, v. 55, p. 347-358, 2014

[5] VENEZIANI, G., et al. Desenvolvimento de simulador aplicados a radiodiagnóstico e radioterapia utilizando impressora 3D. **Pombalina**, Imprensa da Universidade de Coimbra, 2018. Available at: https://digitalis-dsp.uc.pt/bitstream/10316.2/44451/1/Desenvolvimento_de_simulador_aplicados.pdf?ln=pt-pt

[6] BERMAN, B. 3-D printing: The new industrial revolution. **Elsevier,** v. 55, p. 155-162, 2012. Available at: https://www.sciencedirect.com/science/article/pii/S0007681311001790

[7] COSTELLO, J., et al. Incorporating three-dimensional printing into a simulation-based congenital heart disease and critical care training curriculum for resident physicians. **Congenital Heart Disease**, v. 10, p. 185-190, 2015. Available at: https://www.scopus.com/record/display.uri?eid=2-s2.0-84927699615&origin=inward&txGid=3e12b3de6c90d918a44887c29a4980e8

[8] GROSS, C., et al. Evaluation of 3D printing and its potential impact on biotechnology and the chemical sciences. **Anal Chem**, v. 86, p. 3240-3253, 2014.

[9] WEBB, A. A review of rapid prototyping (RP) techniques in the medical and biomedical sector. **Journal of medical engineering & technology,** v. 24, p. 149-153, 2000.

[10] PHARMD, N., et al. Advantages and disadvantages of 3-dimensional printing in surgery: a systematic review. **Elsevier,** v. 159, p. 1485-1500, 2016. Available at: https://www.sciencedirect.com/science/article/pii/S0039606015010557?via%3Dihub.

[11] MATTHEW, D., et al. 3d Printing Of An Aortic Aneurysm To Facilitate Decision Making And Device Selection For Endovascular Aneurysm Repair In Complex Neck Anatomy. J Endovasc Ther, V. 20, P. 863-867, 2013. Available at: Https://Journals.Sagepub.Com/Doi/Full/10.1583/13-4450mr.1

[12] ROSA, M. **Desenvolvimento de um simulador radiográfico homogêneo equivalente ao tórax canino para procedimentos de otimização de imagens radiográficas**. 2015. 22 f. Trabalho de Conclusão de Curso (Bachelor's degree, Medical Physics) - Universidade Estadual Paulista Júlio de Mesquita Filho, Instituto de Biociências de Botucatu, 2015. Available at: http://hdl.handle.net/11449/155074 .

[13] MENDES, S., et al. Development of Object Simulator for Evaluation Periapical Radiographs, in **World Congress on Medical Physics and Biomedical Engineering,** 2015, Toronto, Canada. Annals: Springer Cham, 2015, p. 7-12.

[14] LOUREIRO, M. **Construção de simuladores baseados em elementos de volume a partir de imagens tomográficas coloridas**. 2002. 85 f. Tese (Doctorate degree, Dosimetry and Nuclear Instrumentation) - Universidade Federal de Pernambuco, Pernambuco, 2002. Available at: https://repositorio.ufpe.br/bitstream/123456789/9491/1/arquivo8962_1.pdf.

[15] CORRÊA, R., et al. Efetividade de programa de controle de qualidade em mamografia para o Sistema Único de Saúde. **Rev Saúde Pública**, v. 46, p. 769-76, 2012. Available at: https://www.scielosp.org/scielo.php?pid=S0034-89102012000500002&script=sci_arttext&tlng=pt

[16] VENEZIANI, G., et al. Desenvolvimento de simulador (phantom) de cabeça usando impressora 3D e material tecido equivalente aplicado a medicina veterinária. **Revista Brasileira de Física Médica.** Available at: http://sisconev.com.br/uploads/CBFM2018/20180402183702000000240.pdf.

[17] DeWERD, A., KISSICK, M. The Phantoms of Medical and Health Physics: Devices for research and Development, Wisconsin Institutes for Medical Research. **Springer**, 2014.

[18] MAYER, R., et al. 3D printer generated thorax phantom with mobile tumor for radiation dosimetry. **Review of scientific instruments**, vol. 86 p. 074301-1 – 074301-8 , 2015. Available at: https://www.ncbi.nlm.nih.gov/pubmed/26233396

[19] VENEZIANI, G. R., RODRIGUES, O., SARURABA, R. K., CAMPOS, L. L. Desenvolvimento de simulador aplicados a radiodiagnóstico e radioterapia utilizando impressora 3D. **Radioprotecção**, 2016.

[20] VENEZIANI, G. R., et al. Attenuation coefficient determination of printed ABS and PLA samples in diagnostic radiology standard beams. **Journal of Physics**: Conference Series. v. 733, p. 1-4, 2016.

[21] TRAVASSOS, P., et al. Objeto de teste de baixo custo para radiologia computadorizada. **Revista Brasileira de Física Médica**, v. 6, p. 61-64, 2012. Available at: http://www.rbfm.org.br/rbfm/article/download/186/174.

[22] HARRIS, B., SANNA, N., CHRISTOPHER, M. A feasibility study for using ABS plastic and a low-cost 3D printer for patient-specific brachytherapy mould design. **Australasian physical & engineering sciences in medicine,** v. 38, p. 399-412, 2015.

[23] VICENTE, M., et al. Effect of infill parameters on tensile mechanical behavior in desktop 3D printing. **3D Printing and Additive Manufacturing**, v. 3, p. 183-192, 2016. Available at: https://doi.org/10.1089/3dp.2015.0036.

[24] SAVI, M., et al. Relationship between infill patterns in 3D printing and Hounsfield Unit, in **International Joint Conference RADIO,** 2017, Goiânia.

[25] SAVI, M., ANDRADE, M., POTIENS, M. Comercial filaments testing for use in 3D printed phantoms, in 3º **International Conference on Dosimetry and Applications**, 2019, Lisbon.

[26] TROIANO, M. **Visualização de regiões de ativação cerebral por fMRI sobre volumes multimodais.** 2014. 99 f. Dissertação (Master's degree, Informatics) Universidade Federal do Paraná, Curitiba, 2014. Available at: https://acervodigital.ufpr.br/bitstream/handle/1884/25444/D%20-%20TROIANO,%20MARCELO.pdf?sequence=1

[27] SOUZA, R., et al. Estudo sobre quantificação e classificação dos tecidos biológicos em imagens tomográficas a partir de histogramas. **Revista Brasileira de Física Médica,** v. 4, p. 19-22, 2010. Available at: http://www.rbfm.org.br/rbfm/article/view/71/v4n2p19.

[28] KAIRN, T., CROWE, S., MARKWELL, T. Use of 3D printed materials as tissue-equivalent phantoms. In: **World Congress on Medical Physics and Biomedical Engineering**, 2015, Toronto, Canada. IFMBE Proceedings, vol 51. Springer, Cham.